

ARTICLE

Mechanical force enhanced bony formation in defect implanted with calcium sulphate cement

Jie Zhang, Fan He, Wen Zhang, Meng Zhang, Huilin Yang and Zong-Ping Luo

To improve the osteogenic property of bone repairing materials and to accelerate bone healing are major tasks in bone biomaterials research. The objective of this study was to investigate if the mechanical force could be used to accelerate bone formation in a bony defect *in vivo*. The calcium sulfate cement was implanted into the left distal femoral epiphyses surgically in 16 rats. The half of rats were subjected to external mechanical force via treadmill exercise, the exercise started at day 7 postoperatively for 30 consecutive days and at a constant speed $8 \text{ m} \cdot \text{min}^{-1}$ for $45 \text{ min} \cdot \text{day}^{-1}$, while the rest served as a control. The rats were scanned four times longitudinally after surgery using microcomputed tomography and newly formed bone was evaluated. After sacrificing, the femurs had biomechanical test of three-point bending and histological analysis. The results showed that bone healing under mechanical force were better than the control with residual defect areas of $0.64 \pm 0.19 \text{ mm}^2$ and $1.78 \pm 0.39 \text{ mm}^2$ ($P < 0.001$), and the ultimate loads to failure under mechanical force were $69.56 \pm 4.74 \text{ N}$, stronger than the control with ultimate loads to failure of $59.17 \pm 7.48 \text{ N}$ ($P = 0.039$). This suggests that the mechanical force might be used to improve new bone formation and potentially offer a clinical strategy to accelerate bone healing.

Bone Research (2015) 3, 14048; doi:10.1038/boneres.2014.48; Published online: 20 January 2015

INTRODUCTION

A wide variety of reasons can give rise to bone defects, such as trauma, tumor resection or infection, which has become a challenge in clinical treatment. Filling bone defects not only helps maintain skeletal stability, but also gives the bone a better potential for healing. The clinical demand for excellent bone repairing materials motivated the development of bone biomaterials research in recent years¹ and improving the osteogenic property of bone repairing materials for accelerating bone defect healing is the focus of bone biomaterials research.

Currently, in order to improve the osteogenic property of bone repairing materials, the method of bone tissue engineering through combining osteoconductive carriers together with delivery of osteogenic cells and growth factors has been explored and shows promising results in many studies.^{2–4} However, some failures have also been reported.^{5–6} The efficacy of this engineered method still needs to be further studied and confirmed before clinical application.

It is well known that mechanical force has been proven to play a critical role in bone formation.^{7–10} Bone is a

biological structure adapting optimally to withstanding mechanical stress with minimal materials, described as Wolff's law.¹¹ What's more, mechanical force is a non-invasive and effective means for promoting new bone formation *in vivo*.¹²

In this study, we demonstrated on a rat femur model that the mechanical force could be used as an external promoter to improve new bone formation in the defect implanted with biodegradable bone repairing material. We hypothesized the mild and transient mechanical force stimulation could accelerate bone repair of the defect compared with no force control. The investigation was performed from microCT structural analysis *in vivo*, biomechanical evaluation to histological analysis.

MATERIALS AND METHODS

Animal model

Sixteen 10-week-old female Sprague–Dawley rats were used in the experiment. The rats were acclimatized for 2 weeks in standard cages with regular diet. The experimental protocol was approved by the Institutional Animal Committee.

Material preparation

The bone repairing material studied was calcium sulphate cement (CSC). The calcium sulphate hemihydrate powder (Sigma-Aldrich Co., St Louis, MO, USA) were prepared to $3 \times 3 \text{ mm}^2$ cylindrical samples, using a liquid to powder ratio of 0.5.¹³ The samples were incubated at 37°C for 24 h, and sterilized by gamma irradiation before implantation.

Material implantation

The CSC was implanted into the rats surgically. The rats were anesthetized with 10% chloral hydrate intraperitoneally. A hole (3 mm in diameter and 3 mm in depth) was drilled on the lateral side of the left femur distally underneath the growth plate. After saline irrigation, the holes were carefully dried and implanted with the CSC. Subcutaneous and cutaneous tissues were then closed. Postoperatively, the rats were administered with intramuscular antibiotics for 3 days, had free access to food and water and were monitored daily for any complications or abnormal behaviors.

Mechanical force

The rats were equally divided into a testing group and a control. In the testing group, the mechanical force was applied through a treadmill exercise. The exercise started at day 7 postoperatively for 30 consecutive days and at a constant speed $8 \text{ m}\cdot\text{min}^{-1}$ for $45 \text{ min}\cdot\text{day}^{-1}$.¹⁴ In the control, the rats were restricted in the cages of $47 \times 35 \times 20 \text{ cm}^3$.

MicroCT imaging

The CSC degradation and new bone formation were monitored longitudinally by a microCT scanner *in vivo* on seven rats in each group (SkyScan 1176; Bruker-microCT, Kontich, Belgium). The left distal femur of each rat was scanned at four time points (7, 17, 27 and 37 days). Each rat was anesthetized sustainedly with isoflurane and placed inside the scanner. Each leg was stretched to separate it from the body and scanned along with two phantoms and a tube of water. The most distal end of femur and partial proximal end of tibia were located in a scout view to ensure scanning of the test region. The scanning conditions were kept identical for all the tests ($18 \mu\text{m}$, 65 kV, $380 \mu\text{A}$, 1 mm Al filter, 600 ms exposure). Images were then reconstructed; the same coronary plane on each rat was selected for different time points and the defect area was calculated using the system software.

Biomechanical test

Biomechanical characters were evaluated directly at the terminal point of the experiment (37 days) on the above 14 rats after being euthanized. A three-point bending test of the femur was performed using a microcomputer-controlled electrical universal testing machine (HY-1080;

Hengyi Instrument, Shanghai, China) at a crosshead speed of $1 \text{ mm}\cdot\text{min}^{-1}$. The fixture consisted of a loading pin and two supporting pins. The distance between the two supports was 20 mm. The loading pin compressed the middle of the femur shaft until fracture occurred. The load–displacement curve and the ultimate load were recorded. Besides the two groups tested, two additional groups of femurs ($n=7$) were examined: the intact femurs, and the femurs of defect voids without the CSC.

Histology

The bony structure and CSC remains were examined histologically at the terminal point of the experiment on one rat from each group. After the animals were euthanized, distal femurs were harvested, fixed with 4% paraformaldehyde, dehydrated using graded ethanol series (70%–100%), cleared in toluene and embedded in resin. New bone formation was identified by hematoxylin–eosin staining.

Statistical analyses

Statistical analysis of the defect area from microCT was performed with independent *t*-test, and the difference was considered significant if $P<0.05$. One-way analysis of variance with a significant difference among groups ($P<0.05$) was used to analyze the biomechanical results. The data were further analyzed by Turkey's *post-hoc* multiple comparisons test.

RESULTS

MicroCT imaging

MicroCT reconstruction showed that the new bone formation was enhanced by external mechanical force (Figures 1 and 2). At day 7 when loading started, the difference in the

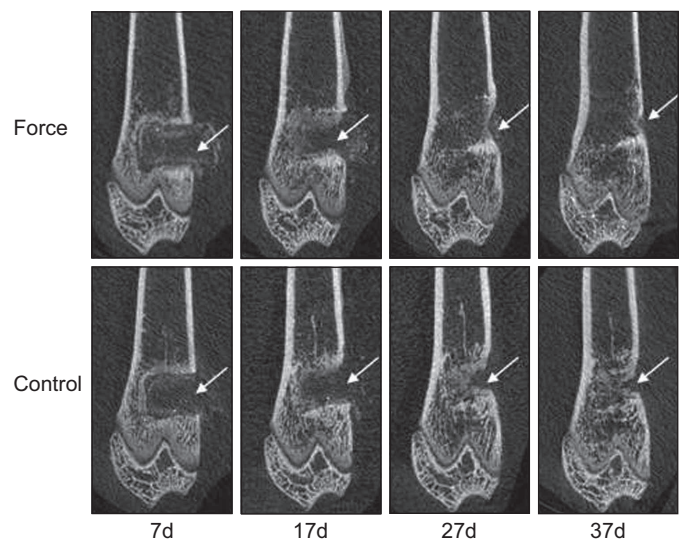


Figure 1. The microCT images showing the new bone formation are enhanced by the mechanical force.

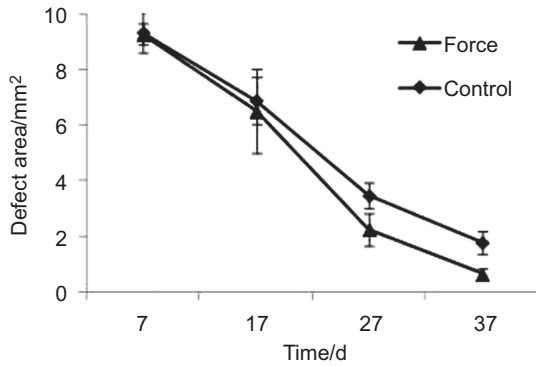


Figure 2. The defect area which diminishes over time.

CSC filled defect area was not significant between two groups: $9.28 \pm 0.36 \text{ mm}^2$ in the mechanical force group and $9.34 \pm 0.74 \text{ mm}^2$ in the control, respectively ($P=0.859$). At day 17, the defect area shrank in both the mechanical force ($6.50 \pm 1.52 \text{ mm}^2$) and the control ($6.75 \pm 1.07 \text{ mm}^2$) groups, but the difference was not significant ($P=0.542$). At day 27, the mechanical force group showed significant reduction of the defect area ($2.25 \pm 0.58 \text{ mm}^2$) compared with the control group ($3.47 \pm 0.45 \text{ mm}^2$) ($P=0.002$). At day 37, the defect area of the mechanical force group ($0.64 \pm 0.19 \text{ mm}^2$) is significantly different with that of the control group ($1.78 \pm 0.39 \text{ mm}^2$) ($P<0.001$).

Biomechanical test

The three-point bending test at day 37 illustrated that the mechanical force group with the ultimate load to failure of $69.56 \pm 4.74 \text{ N}$ was significantly stronger than the control with the ultimate load to failure of $59.17 \pm 7.48 \text{ N}$ ($P=0.039$). However, the femur strength of the mechanical force group is significantly weaker than that of intact femur group ($80.46 \pm 2.79 \text{ N}$) ($P=0.028$) (Figures 3 and 4). In addition, the ultimate loads to failure of the two groups were significantly stronger than the void group ($43.38 \pm 7.48 \text{ N}$) ($P=0.001$).

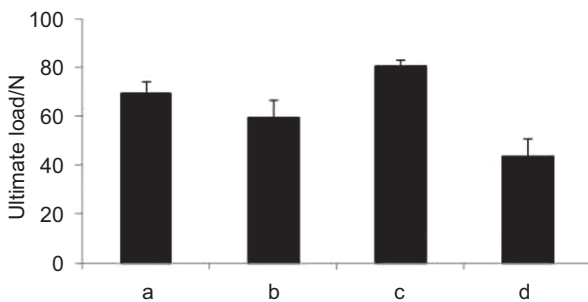


Figure 3. The ultimate load to failure of the femur under the three-point bending test: (a) the mechanical force; (b) the control; (c) the intact femur; (d) the femur with void.

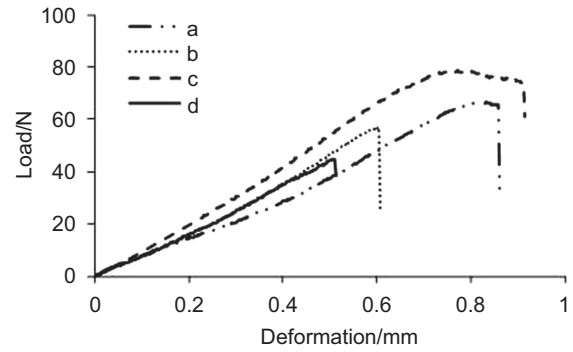


Figure 4. Typical load-deformation curves from the three-point bending test: (a) the mechanical force; (b) the control; (c) the intact femur; (d) the femur with void.

Histology

The histological results at day 37 confirmed the microCT finding of better new bone formation by the mechanical force (Figure 5). The orange is the new bone formed in the defect, and the purple is the nucleus of bone cells including osteoblasts, osteoclasts and osteocytes. The blank part within the black curve is nothing. Both groups showed complete CSC degradation. However, the residue area of the defect with mechanical stimulation was 0.76 mm^2 , smaller than that in control (1.48 mm^2).

DISCUSSION

To improve the osteogenic property of bone repairing materials for accelerating bone healing is the focus of bone biomaterial research, which reduces the time of bone healing and allows patients a quicker return to normal activity. It has long been known that bone adapts according to the local mechanical environment and external mechanical force has a positive effect on bone formation.⁷⁻¹⁰ In this study, we try to investigate the effect of mild mechanical force on the osteogenic property of biodegradable bone repairing material. Our results demonstrated that mechanical force could improve the

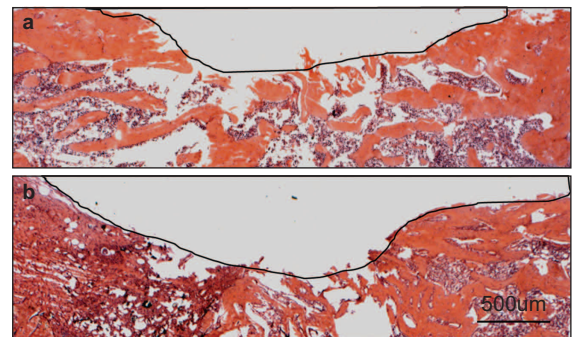


Figure 5. The hematoxylin-eosin staining of the defect area at the terminal point of day 37: (a) the mechanical force; (b) the control. The residue defect area was highlighted with the black curve.

osteogenic property of bone repairing material and enhance bone formation of the defect.

In the field of bone tissue engineering, some methods have been developed and successful to some extent. One of the most extensively studied methods is to combine osteoconductive carriers with bone morphogenetic proteins (BMPs). BMPs act locally and therefore must be delivered directly to the site of fracture via a carrier, and the question remains that the release kinetics of BMPs in the fracture site still be unsuccessfully controllable and will be affected by the degradation rate of the carrier. Furthermore, some carriers have been shown unsuitable for transferring BMPs^{5–6} and the excellent carrier is still under searching.

In contrast, the mechanical force stimulation has proven to be safe and effective. The primary advantage of mechanical intervention is the clinical implementation: the mechanical force can be readily applied via external loading devices such as a mechanical vibration system or physical exercises.

In this study, our results show mechanical force could improve the osteogenic property of bone repairing material and enhance bony formation, which is consistent with the previous study.¹⁵ Interestingly, at the early stage (the first 10 days after loading started) of bone healing, the defect area of the mechanical force group is not significantly different from that of the control group, revealing that mechanical force did not play the role of promoting bone formation. One possible explanation is that the defect site was filled with the bone repairing material making no room for new bone to form. But at the rest of experiment, mechanical force obviously promotes bone formation and accelerates bone repair. Although the mechanism by which bone responds to mechanical force was not studied here, substantial biomechanical researches had advanced the understanding of the cellular and molecular mechanism of bone adaptation. The mechanisms for bone adaptation involve a multistep process of cellular mechanotransduction. Firstly, the external mechanical force should convert to local mechanical signals *in vivo*, such as fluid flow stresses, which initiate a response by sensor cells (predominantly osteocytes and bone lining cells).^{16–17} Secondly, the local mechanical signals transform into biochemical signaling molecules such as the prostaglandins and nitric oxide produced by sensor cells^{18–21}. Thirdly, these signaling molecules must signal to effector cells (osteoblasts or osteoclasts). Nitric oxide and prostaglandin have been shown to be the two main potent factors in bone maintenance and remodeling by inhibiting osteoclast resorptive activity and stimulating the number of osteoblasts.^{22–26} Lastly, appropriate and substantial architectural changes will occur. In addition, bone gain induced by mechanical force may be tightly related to vascular

endothelial growth factor-mediated bone angiogenesis and angiogenesis is essential for bone healing. Upregulation of vascular endothelial growth factor was detected after 10 days of treadmill exercise, but vascular endothelial growth factor blockade in 5-week trained rats fully prevented the exercise-induced increase in bone formation.²⁷ Nevertheless, the mechanisms of mechanical force-induced bone formation and remodeling are very complex and profound, which need to be further investigated.

A few critical parameters used in the study deserve in-depth discussion: (i) the timing of applying mechanical force. Application of mechanical force started at day 7. This was because loading immediately after surgery could inhibit bone and soft tissue healing or disrupt early blood vessel ingrowth into the hematoma;^{28–33} (ii) the force magnitude. The treadmill speed for the mechanical force used was $8 \text{ m} \cdot \text{min}^{-1}$, which was identical to the one reported in literature.¹³ This speed was at a pace of mild walking of 0.73 Hz; (iii) The use of CSC. The main reason to use CSC was its relatively fast degradation of 4–8 weeks *in vivo*.^{34–37} This degradation time was similar to the time of murine bone turnover.³⁸

The limitations of this study included that biomechanical and histological results were only reported at the terminal point of testing. The study relied primarily on the non-destructive microCT to evaluate the bone formation in the defect.³⁹ Future biomechanical and histological studies can be done with more samples at different periods of time to gain additional information.

In conclusion, external mechanical force could be used as a promoter to improve the osteogenic property of bone repairing material and enhance bone healing. This suggests that the mechanical force might be used to improve the new bone formation and potentially offer a clinical strategy to accelerate bone healing. More researches are needed to characterize the effect of mechanical force on bone repair and regeneration.

Competing interests

The authors declare no conflict of interest.

Acknowledgements

This work was supported in part by the Natural Science Foundation of China under the grants of 11072165, 31270995 and 81320108018.

References

- Porter JR, Ruckh TT, Popat KC. Bone tissue engineering: a review in bone biomimetics and drug delivery strategies. *Biotechnol Prog* 2009; **25**: 1539–1560.
- Young S, Patel ZS, Kretlow JD *et al*. Does effect of dual delivery of vascular endothelial growth factor and bone morphogenetic protein-2 on bone regeneration in a rat critical-size defect model. *Tissue Eng Part A* 2009; **15**: 1.
- Patel ZS, Young S, Tabata Y, Jansen JA, Wong M, Mikos AG. Dual delivery of an angiogenic and osteogenic growth factor for bone regeneration in a critical size defect model. *Bone* 2008; **43**: 931.

- 4 Kanczler JM, Oreffo RO. Osteogenesis and angiogenesis: the potential for engineering bone. *Eur Cell Mater* 2008; **15**: 100–114.
- 5 Meikle MC, Papaioannou S, Ratledge TJ *et al*. Effect of poly DL-lactide-co-glycolide implants and xenogeneic bone matrix-derived growth factors on calvarial bone repair in the rabbit. *Biomaterials* 1994; **15**: 513–521.
- 6 Seto I, Asahina I, Oda M, Enomoto S. Reconstruction of the primate mandible with a combination graft of recombinant human bone morphogenetic protein 2 and bone marrow. *J Oral Maxillofac Surg* 2001; **59**: 53–61.
- 7 Bass SL, Saxon L, Daly RM *et al*. The effect of mechanical loading on the size and shape of bone in pre-, peri-, and postpubertal girls: a study in tennis players. *J Bone Miner Res* 2002; **17**: 2274–2280.
- 8 Dodge T, Wanis M, Ayoub R *et al*. Mechanical loading, damping, and load-driven bone formation in mouse tibiae. *Bone* 2012; **51**: 810–818.
- 9 Chen HH, Morrey BF, An KN, Luo ZP. Bone remodeling characteristics of a short-stemmed total hip replacement. *J Arthroplasty* 2009; **24**: 945–950.
- 10 Westerlind KC, Wronski TJ, Ritman EL *et al*. Estrogen regulates the rate of bone turnover but bone balance in ovariectomized rats is modulated by prevailing mechanical strain. *Proc Natl Acad Sci USA* 1997; **94**: 4199–4204.
- 11 Chen JH, Liu C, You L, Simmons CA. Boning up on Wolff's Law: mechanical regulation of the cells that make and maintain bone. *J Biomech* 2010; **43**: 108–118.
- 12 Ferreri SL, Talish R, Trandafir T, Qin YX. Mitigation of bone loss with ultrasound induced dynamic mechanical signals in an OVX induced rat model of osteopenia. *Bone* 2011; **48**: 1095–1102.
- 13 Dewi AH, Ana ID, Wolke J, Jansen J. Behavior of plaster of Paris-calcium carbonate composite as bone substitute. A study in rats. *J Biomed Mater Res A* 2013; **101**: 2143–2150.
- 14 Oxlund H, Andersen NB, Ørtoft G, Ørskov H, Andreassen TT. Growth hormone and mild exercise in combination markedly enhance cortical bone formation and strength in old rats. *Endocrinology* 1998; **139**: 1899–1904.
- 15 Roshan-Ghias A, Terrier A, Bourban PE, Pioletti DP. *In vivo* cyclic loading as a potent stimulatory signal for bone formation inside tissue engineering scaffold. *Eur Cell Mater* 2010; **19**: 41–49.
- 16 Reich KM, Gay CV, Frangos JA. Fluid shear stress as a mediator of osteoblast cyclic adenosine monophosphate production. *J Cell Physiol* 1990; **143**: 100–104.
- 17 Turner CH, Forwood MR, Otter MW. Mechanotransduction in bone: do bone cells act as sensors of fluid flow? *FASEB J* 1994; **8**: 875–878.
- 18 Johnson DL, McAllister TN, Frangos JA. Fluid flow stimulates rapid and continuous release of nitric oxide in osteoblasts. *Am J Physiol* 1996; **271**: E205–E208.
- 19 Klein-Nulend J, Burger EH, Semeins CM, Raisz LG, Pilbeam CC. Pulsating fluid flow stimulates prostaglandin release and inducible prostaglandin G/H synthase mRNA expression in primary mice bone cells. *J Bone Miner Res* 1997; **12**: 45–51.
- 20 Pitsillides AA, Rawlinson SC, Suswillo RF, Bourrin S, Zaman G, Lanyon LE. Mechanical strain-induced NO production by bone cells: a possible role in adaptive bone (re)modeling? *FASEB J* 1995; **9**: 1614–1622.
- 21 Somjen D, Binderman I, Berger E, Harell A. Bone remodeling induced by physical stress is prostaglandin E2 mediated. *Biochim Biophys Acta* 1980; **627**: 91–100.
- 22 Kasten TP, Collin-Osdoby P, Patel N *et al*. Potentiation of osteoclast bone-resorption activity by inhibition of nitric oxide synthase. *Proc Natl Acad Sci USA* 1994; **91**: 3569–3573.
- 23 MacIntyre I, Zaidi M, Alam AS *et al*. Osteoclastic inhibition: an action of nitric oxide not mediated by cyclic GMP. *Proc Natl Acad Sci USA* 1991; **88**: 2936–2940.
- 24 Riancho JA, Salas E, Zarrabeitia MT *et al*. Expression and functional role of nitric oxide synthase in osteoblast-like cells. *J Bone Miner Res* 1995; **10**: 439–446.
- 25 Riancho JA, Zarrabeitia MT, Fernandez-Luna JL, Gonzalez-Macias J. Mechanisms controlling nitric oxide synthesis in osteoblasts. *Mol Cell Endocrinol* 1995; **107**: 87–92.
- 26 Imamura K, Ozawa H, Hiraide T *et al*. Continuously applied compressive pressure induces bone resorption by a mechanism involving prostaglandin E2 synthesis. *J Cell Physiol* 1990; **142**: 177–185.
- 27 Yao Z, Lafage-Proust MH, Plouët J, Bloomfield S, Alexandre C, Vico L. Increase of both angiogenesis and bone mass in response to exercise depends on VEGF. *J Bone Miner Res* 2004; **19**: 1471–1480.
- 28 Gardner MJ, van der Meulen MC, Demetrakopoulos D, Wright TM, Myers ER, Bostrom MP. *In vivo* cyclic axial compression affects bone healing in the mouse tibia. *J Orthop Res* 2006; **24**: 1679–1686.
- 29 Claes L, Eckert-Hübner K, Augat P. The effect of mechanical stability on local vascularization and tissue differentiation in callus healing. *J Orthop Res* 2002; **20**: 1099–1105.
- 30 Goodship AE, Cunningham JL, Kenwright J. Strain rate and timing of stimulation in mechanical modulation of fracture healing. *Clin Orthop Relat Res* 1998; **355**: S105–S115.
- 31 Hente R, Cordey J, Rahn BA, Maghsudi M, von Gumpfenberg S, Perren SM. Fracture healing of the sheep tibia treated using a unilateral external fixator. Comparison of static and dynamic fixation. *Injury* 1999; **30 Suppl 1**: A44–A51.
- 32 Wolf JW, White AA, Panjabi MM, Southwick WO. Comparison of cyclic loading versus constant compression in the treatment of long-bone fractures in rabbits. *J Bone Joint Surg* 1981; **63**: 805–810.
- 33 Wallace AL, Draper ERC, Strachan RK, McCarthy ID, Hughes SPF. The vascular response to fracture micromovement. *Clin Orthop Relat Res* 1994; **301**: 281–290.
- 34 Turner TM, Urban RM, Gitelis S, Kuo KN, Andersson GB. Radiographic and histologic assessment of calcium sulfate in experimental animal models and clinical use as a resorbable bone-graft substitute, a bone-graft expander, and a method for local antibiotic delivery. One institution's experience. *J Bone Joint Surg Am* 2001; **83-A Suppl 2**(Pt 1): 8–18.
- 35 Glazer PA, Spencer UM, Alkalay RN, Schwarzt J. *In vivo* evaluation of calcium sulfate as a bone graft substitute for lumbar spinal fusion. *Spine J* 2001; **1**: 395–401.
- 36 Tay BK, Patel VV, Bradford DS. Calcium sulfate- and calcium phosphate-based bone substitutes. Mimicry of the mineral phase of bone. *Orthop Clin North Am* 1999; **30**: 615–623.
- 37 Murashima Y, Yoshikawa G, Wadachi R, Sawada N, Suda H. Calcium sulphate as a bone substitute for various osseous defects in conjunction with apicectomy. *Int Endod J* 2002; **35**: 768–774.
- 38 Melo LG, Nagata MJ, Bosco AF, Ribeiro LL, Leite CM. Bone healing in surgically created defects treated with either bioactive glass particles, a calcium sulfate barrier, or a combination of both materials. A histological and histometric study in rat tibias. *Clin Oral Implants Res* 2005; **16**: 683–691.
- 39 Schulte FA, Lambers FM, Kuhn G, Müller R. *In vivo* micro-computed tomography allows direct three-dimensional quantification of both bone formation and bone resorption parameters using time-lapsed imaging. *Bone* 2011; **48**: 433–442.



This work is licensed under a Creative Commons Attribution-NonCommercial-ShareAlike 3.0 Unported License. The images or other third party material in this article are included in the article's Creative Commons license, unless indicated otherwise in the credit line; if the material is not included under the Creative Commons license, users will need to obtain permission from the license holder to reproduce the material. To view a copy of this license, visit <http://creativecommons.org/licenses/by-nc-sa/3.0/>